Second harmonic generation of high peak power, high repetition rate from Yb-doped fiber amplifier

Hiroaki Sunaga, Ryusuke Horiuchi, Kazuya Jyosui, Kazuyoku Tei, Shigeru Yamaguchi, Kenzo Nanri, and Tomoo Fujioka

Department of Physics, Tokai University, 1117 Kitakaname Hiratuka-shi Kanagawa 259-1292, Japan

A high peak power, high repetition rate master oscillator power amplifier (MOPA) system incorporating an Yb-doped fiber amplifier and its second harmonic generation (SHG) were investigated in detail. The oscillator is actively Q-switched microchip laser at repetition rate of 50 kHz with a pulse width of 2.8 ns. The amplifier employing Yb-doped polarization maintaining fiber and having a large mode area was excited by a laser diode with an optical power of 17 W. As results, the amplified average output power of 10 W and optical-optical conversion efficiency of 59% were achieved. In this MOPA system, experiments were performed by using KTP and LBO crystals. The conversion efficiency of 21% and 40%, SHG maximum power of 0.92 and 3.3 W were obtained for KTP and LBO crystals respectively.

OCIS codes: 190.2620, 060.2320, 140.4480.

Nanosecond high peak power sources of near-infrared, visible and ultraviolet radiation are expected for industry, and medical applications[1]. Especially high repetition, short pulse laser is requested from industrial. The Yb-doped fiber master oscillator power amplifier (MOPA) system, which can generate high peak power and high repetition rate pulses, and has many other advantages, such as vibration-proof, compactness and water free for cooling[2,3], has been attractive for industrial micro-machining[4]. In our system, a compact actively Q-switched microchip laser is amplified in an Yb-doped fiber. The gain material of the microchip laser is Nd:YVO_4 which ensures high gain and short pulse width at higher repetition rate. The seed pulse of wavelength 1064 nm is amplified in the Yb-doped double-clad fiber, which has the emission of Yb-ion from 1000 to 1100 nm. The upper limit of peak power in a fiber amplifier is determined by the fiber nonlinearities, such as stimulated Brillouin scattering (SBS), stimulated Raman scattering (SRS) and self-focusing[5−7]. The increased mode area of double-clad fiber pushes up the limit of peak power limited by the above fiber nonlinearities.

In this paper, the amplification characteristic of Yb-doped fiber MOPA system is studied, and the second harmonic generation (SHG) (532 nm) efficiencies by using KTP and LBO crystal are compared. The mismatching influence of the self phase modulation (SPM) in fiber on SHG is also discussed.

Figure 1 shows the Yb-doped fiber MOPA system and

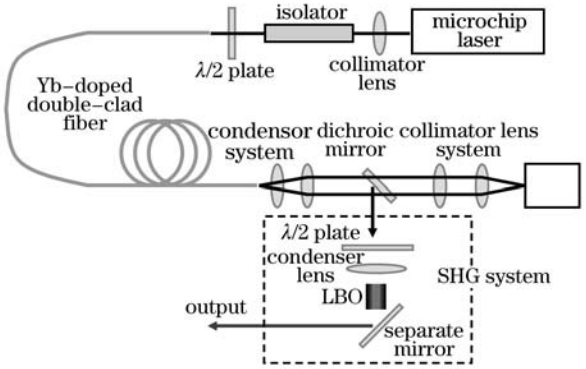

Fig. 1. Schematic diagram of the optical system.

SHG. For the present experiment, the fiber amplifier was seeded with the 1064-nm output of the Q-switched Nd:YVO_4 microchip laser, which was pumped by an 808-nm diode laser. The seed light produced with a nearly Gaussian temporal profile (2.8 ns, full width at half maximum (FWHM)) and an pulse energy of 9.4 μJ at a repetition rate of 50 kHz.

The Yb-doped polarization maintaining double-clad fiber is used as the gain material. The high pulse energy and peak power were enabled by the use of large mode area core fiber. The Yb-doped fiber had a core diameter of 30 μm, numerical aperture of 0.06. The Yb-doped fiber was pumped by a laser diode operated at wavelength of 978 nm and output of 17 W. The seed pulse and pump light were counter-propagating[8].

The second harmonic (532 nm) of the amplifier output was generated by KTP and LBO crystals. The KTP crystal was arranged at the position with a beam waist radius of 162.4 μm. The critical phase matching of type II ($\theta = 90°$, $\varphi = 23.5°$) was selected for KTP, and its size was 5×5×10 (mm). The LBO crystal was arranged at the position with a beam waist radius of 66.2 μm and the temperature was maintained at 148°C. The non-critical phase matching of type I ($\theta = 90°$, $\varphi = 0°$) was selected for LBO. The size was 3×3×10 (mm). The proper polarization orientation was selected by $\lambda/2$ plate.

Figure 2 shows the amplification characteristic of Yb-doped fiber MOPA system of 1064 nm. When the fiber was pumped by the maximum LD power of 17 W, the amplified output power of 10 W was obtained with the optical-optical efficiency of 59%. The corresponding peak power was 71.4 kW. In this case, the average input power of seed pulses was 0.33 W. The limit of maximum peak power is decided by nonlinear effects in fiber rather than optical damage in our case. SRS limits the peak power as well.

The threshold power in relation with SRS that occurs in fibers can be approximated as

$$P_{\mathrm{SRS}} \approx \frac{16A_{\mathrm{eff}}}{Kg_{\mathrm{R}}L_{\mathrm{eff}}}, \tag{1}$$

where g_{R} is Raman gain, A_{eff} is the effective mode field area, L_{eff} is the effective fiber length and K is the polarization dependence factor[9,10]. It is assumed that

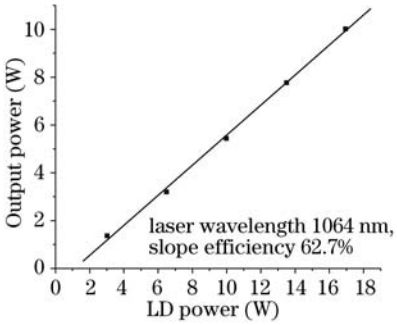

Fig. 2. Fiber amplifier output power versus laser diode (LD) power. Solid line is the linear fit for experimental results.

the absorption length effective is equal to fiber length, because there is absorption of pump light in fiber core. The effective fiber length can be approximated as

$$L_{\text{eff}} = \frac{1}{\alpha_{\text{P}}}[1 - \exp(-\alpha_{\text{P}}\text{L})], \tag{2}$$

where α_{P} is absorption coefficient of pump light. The effective fiber length and SRS threshold in the actual experimental condition were estimated as 720 mm and 157 kW. In the vicinity of the 1115-nm wavelength (Raman frequency shift Ω_{SRS} ~13.5 THz), the Stokes component was not confirmed.

Figure 3 shows the pulse shape of the seed pulse and amplified pulse. The solid line is the pulse shape of the seed pulse after passing the fiber, and the dotted line is the amplified pulse. The wave profile of the seed pulse looks similar to the amplified pulse, and both FWHMs are 2.8 ns at the repetition frequency of 50 kHz.

Figure 4 shows the relation of the SHG output and peak intensity in each crystal. For the KTP crystal, the SHG maximum output power of 0.92 W was obtained at the intensity of 58.6 MW/cm^2. For LBO, the SHG maximum output power of 3.3 W was obtained at the intensity of 435 MW/cm^2. The crystal damage was not found in the vicinity of damage threshold in the two crystals. Figures 5 and 6 show the SHG conversion efficiency and mismatch as a function of the intensity for crystals in the SHG stage and as a function of the intensity in the fiber core. For the case of KTP, SHG efficiency increases up to near the intensity of 20 MW/cm^2 for KTP crystal (2 GW/cm^2 in fiber), and the mismatch does not increase too much. At the intensity of 20 MW/cm^2 for KTP crystal (2 GW/cm^2 in fiber), the SHG conversion efficiency of 21% was obtained. At higher intensity than 20 MW/cm^2 for KTP crystal (2 GW/cm^2 in fiber), SHG efficiencies begin to fall gradually and the mismatch is still increasing. Mismatch ΔkL from the SHG efficiencies in the actual experiment was calculated as

$$\Delta kL = \gamma SN^2(\mu, \gamma), \tag{3}$$

here $SN(\mu, \gamma)$ is the elliptic two-parametric sine (a tabulated special Jacoby function). μ was calculated as

$$\mu = \left[\sqrt{1 + \left(\frac{\Delta KL}{4}\right)^2 \left(\frac{L_{\text{NL}}}{L}\right)^2} - \frac{\Delta KL}{4}\frac{L_{\text{NL}}}{L}\right]\frac{L}{L_{\text{NL}}}, \tag{4}$$

and γ was calculated as

$$\gamma = \left[\sqrt{1 + \left(\frac{\Delta KL}{4}\right)^2 \left(\frac{L_{\text{NL}}}{L}\right)^2} - \frac{\Delta KL}{4}\frac{L_{\text{NL}}}{L}\right]^2, \tag{5}$$

where L_{NL} is the length of nonlinear crystal that would produce a conversion efficiency and L is the length of nonlinear crystal[11]. For the LBO crystal, the SHG maximum conversion efficiency of 40% was obtained. Mismatch of LBO crystal was smaller than in KTP crystal and SHG conversion efficiency of LBO crystal was larger than in KTP crystal.

The spectral broadening by SPM is thought to be the cause why the SHG efficiencies are lower than expected. The spectrum in the experiment is shown in Fig. 7.

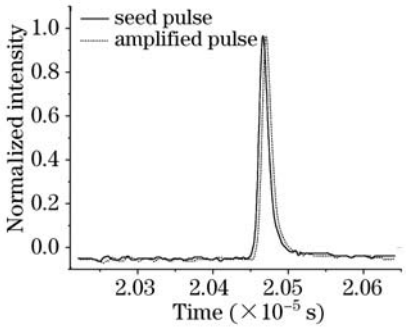

Fig. 3. Amplified pulse shape.

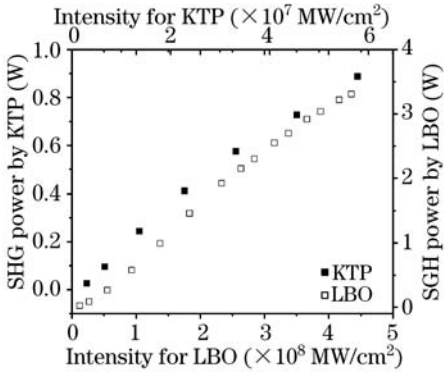

Fig. 4. Intensity for nonlinear crystal versus SHG power.

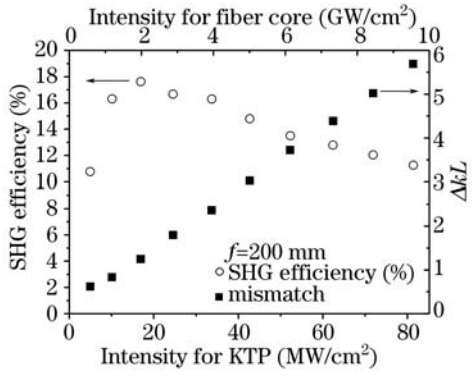

Fig. 5. SHG efficiency and mismatch changing with intensity for KTP crystal and fiber core.

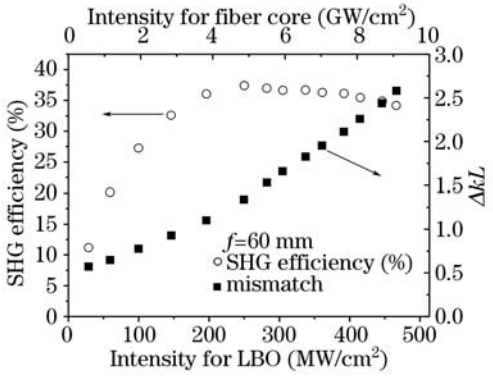

Fig. 6. SHG efficiency and mismatch changing with intensity for LBO crystal and fiber core.

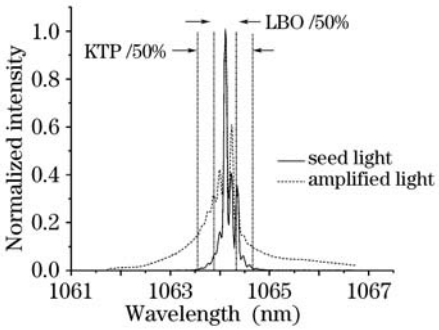

Fig. 7. Normalized optical spectrum of seed pulse and amplified pulse output. Seed output power was 0.33 W. Amplified output power was 10 W.

The solid line is the spectrum of seed pulse and the dotted line is the spectrum of amplified pulse with the peak power of 71.4 kW. The spectral bandwidths in the frequency conversion are decided by the crystal. The spectral bandwidth of the KTP crystal is 0.45 nm and for the LBO crystal it is 1.1 nm. The spectrum of amplified pulse is distributed across the spectral bandwidth of LBO in Fig. 7.

The extension of the spectrum by frequency chirp was shown in Fig. 8. The solid line is a theoretical value of the maximum chirp corresponding to the peak power. The theoretical entire frequency chirp with the peak power of 71.4 kW was approximated as

$$\Delta\omega_{\max} = 0.86\Delta\omega\phi_{\max}, \tag{6}$$

where $\Delta\omega$ is the FWHM and $\phi_{\max}$ is the maximum nonlinear phase shift. The latter was approximated as

$$\phi_{\max} = \gamma P_0 z_{\text{eff}}, \tag{7}$$

where γ is the nonlinear coefficient, P_0 is the peak power and z_{eff} is the effective fiber length (effective propagation length)[12]. γ was calculated by using nonlinear refractive index, center frequency, velocity of light and effective mode area. The dotted line in Fig. 8 is a mended line in the half-frequency of the spectral bandwidths of the KTP crystal. The two-point broken line is about LBO crystal. Each of four plots shows the frequency shift from the spectrum of amplified pulse at each spectrum intensity

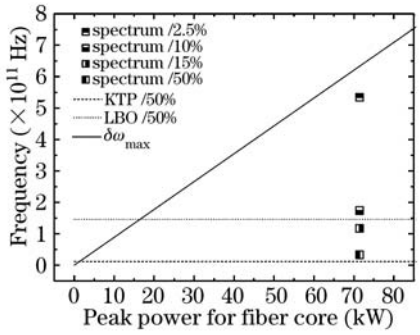

Fig. 8. Frequency shift by SPM during fiber amplifying.

in Fig. 7. The component with the spectrum intensity less than 10% of the peak is distributed out of the bandwidth of LBO and generated by SPM. According to the theory of nonlinear effect in fiber, the frequency chirp (spectral broadening) increases along with the FWHM of the seed spectrum, interaction length of the fiber, and nonlinear coefficient. Therefore, by reducing the spectral broadening, a higher efficiency of frequency conversion can be expected by shortening the length of the fiber and narrowing of the line width of the oscillator. It is necessary to select the fiber with a high absorption cladding to shorten the fiber length.

We developed an Yb-doped fiber MOPA system, and the second harmonic was generated. The Yb-doped fiber MOPA system was operated at the peak power of 71.4 kW with repetition rate of 50 kHz and slope efficiency of 62.7%. The peak power and LD power were limited by SRS. The pulse shape did not change before and after amplification. In SHG, the LBO crystal was able to improve the conversion efficiencies more effectively than the KTP crystal. Moreover, it was shown that narrowing of the line width of the oscillator and choosing the fiber with a high absorption cladding to shorten the fiber length are thought to be effective to reduce the frequency shift by SPM. In the future work will be done to improve the SHG conversion efficiency and power, and research higher harmonics generation.

H. Sunaga's e-mail address is 5asnm013@keyaki.cc.u-tokai.ac.jp.

References

1. A.V. Kliner, F. D. Teodoro, P. Koplow, W. Moore, and A. V. Smith, Opt. Commun. **210,** 393 (2002).
2. Y. H. Tsang, T. A. King, D. Ko, and J. Lee, Opt. Commun. **259,** 236 (2006).
3. F. D. Teodoro and P. R. Hoffman, Opt Commun. **252,** 111 (2005).
4. T. J. Kane, L. A. Smoliar, F. Adams, M. A. Arbore, D. R. Balsley, M. W. Byer, G. E. Conway, W. M. Grossman, G. Keaton, J. D. Kmetec, M. Leonardo, J. J. Morehead, and W. Wiechmann, Proc. SPIE **5662,** 496 (2004).
5. Y. Jaouen, G. Canat, S. Grot, and S. Bordais, Comptes Rendus Physique **7,** 163 (2006).
6. Y. Wang, IEEE J. Quantum Electron. **41,** 779 (2005).
7. Y. Wang, J. Lightwave Technol. **23,** 2139 (2005).
8. F. D. Teodoro and C. D. Brooks, Proc. SPIE **6102,** 61020K (2006).

9. W. Torruellas, Y. Chen, B. McIntosh, J. Farroni, K. Tankala, S. Webster, D. Hagan, M. J. Soileau, M. Messerly, and J. Dawson, Proc. SPIE **6102,** 61020N (2006).
10. R. L. Farrow, D. A. V. Klinear, P. E. Schrader, A. A. Hoops, S. W. Moore, G. R. Hadley, and R. L. Schmitt, Proc. SPIE **6102,** 61020L (2006).
11. R. L. Sutherland, *Handbook of Nonlinear Optics* (2nd edn.) (Marcel Dekker, New York, 2003).
12. G. P. Agrawal, *Nonlinear Fiber Optics* (2nd edn.) (Academic Press, San Diego, 1995).